doi.org/10.36721/PJPS.2025.38.4.REG.13523.1

Novel strategy for AAV vector design in gene therapy and its biosafety assessment

Caihong Gao
School of Life Sciences Fudan University Shanghai, Shanghai, China

Abstract: To develop a novel AAV vector design for gene therapy by synthesizing the AAVITR microcarrier sequence, constructing and identifying the amplification plasmid, and evaluating the properties of the microcarrier prepared by heat denaturation. We also assess the biosafety of this new vector by examining its toxicity, immunogenicity, and potential for immune cell infiltration. The AAVITR micro carrier sequence was designed and synthesized, followed by the construction of an amplification plasmid to express the vector sequence and the identification of pUC57-minivector. The *in vitro* expression of the AAVITR micro carrier was analyzed and its safety was assessed through toxicity, immunogenicity, and immune cell infiltration assays. In safety assessments, the new vector demonstrated superior survival and apoptosis rates compared to conventional vectors. Additionally, the AAV-ITR micro carrier showed significant advantages in immune cell infiltration, cytokine levels, and antibody production, indicating a potent immune response. The novel AAVITR micro vector developed in this study offers improved safety and efficacy in gene therapy, with notable advantages in immune response and biosafety, providing a promising alternative to traditional AAV vectors.

Keywords: AAV vector, safety assessment, immune response, cytokines, antibody production

Submitted on 07-10-2024 – Revised on 05-12-2024 – Accepted on 04-03-2025

INTRODUCTION

Adeno-associated virus (AAV) is a member of the Dependovirus genus within the family of small viruses and is recognized as one of the smallest known virus species. AAV has the capacity to establish both productive infections in the presence of helper viruses, such as adenoviruses or herpes simplex viruses, and nonproliferative latent infections in various cell types in the absence of a helper virus. While most adults exhibit evidence of AAV infection, it is widely accepted that AAV is not a pathogenic agent and does not cause any known human diseases. Among the numerous AAV serotypes, AAV type 2 is the most extensively studied and serves as a representative example of AAV characteristics.

Gene therapy represents a promising therapeutic modality with the potential to cure many previously intractable diseases (Li and Samulski, 2020; Bulcha *et al*., 2021). AAV vectors are particularly valuable in this field due to their low immunogenicity, high transfection efficiency, and ability to support long-term stable gene expression. Despite these advantages, traditional AAV vectors encounter unresolved challenges in practical applications, necessitating ongoing research into innovative design strategies to improve their performance and safety (Pupo *et al*., 2022; Zu and Gao, 2021).

This study introduces a novel strategy for AAV vector design in gene therapy, focusing on reducing immunogenicity, enhancing transfection efficiency, and bolstering biosafety. We have successfully designed and synthesized AAVITR micro vector sequences and constructed amplification plasmids for AAVITR gene expression micro vectors. Our approach involves the preparation and characterization of AAVITR micro vectors, denoted as pUC57-minivecto and the assessment of the *in vitro* expression. The safety of these vectors was evaluated through cytotoxicity, immunogenicity and immune cell infiltration assays. Cytotoxicity assessment included the measurement of cell survival rate, apoptosis rate, and morphological changes. Immunogenicity was determined by monitoring cytokine levels and IgG antibody production, while immune cell infiltration was assessed by examining the number and distribution of immune cells in tissue sections.

Furthermore, this paper details the identification tests conducted across four key areas: The construction and identification of plasmids, the construction and identification of AAVITR gene episomal micro carrier amplification plasmids, the preparation and identification of AAVITR gene episomal micro carriers and the expression of AAV-ITR gene episomal microcarriers in 293T cells. These tests provide a foundational basis for the future development of mutant libraries and extensive screening of mutants, contributing to the advancement of AAV vector design in gene therapy.

Related works

As gene therapy has been widely used in clinical trials, many scholars have begun to study AAV vectors in gene therapy. Researchers in the literature (Zhao *et al.*, 2020) pointed out that the conventional production method of AAV vectors is co-transfection of HEK293 cells with

**Corresponding author:* e-mail: vivian202408@126.com

three plasmids, and among the current large-scale AAV production systems, the system that relies on baculoviral expression vectors to infect insect cells for the production of AAV viruses has been widely used, which has the unique advantages of high infectious efficiency, BEV non-pathogenicity and low cost. Literature (Zhao *et al.*, 2022) established the first generation Bac system for AAV production, which has only one bacterial artificial chromosome vector carrying the rep and cap genes required for AAV production, acting for virus replication and capsid protein synthesis. In literature (Au *et al.*, 2022) researchers pointed out that directed evolution is a high-throughput genetic engineering method that generates high abundance mutation libraries by mimicking the process of natural evolution using random point mutation method, in vitro recombination and random sequence peptide display. The libraries are subjected to selection pressure according to specific purposes, and genetic screening is performed iteratively to enrich for effective mutants.

In their study, the researchers of literature (Ghosh *et al.*, 2020) concluded that the application of directed evolutionary strategies allows for iterative optimization of AAV Cap genes, resulting in novel AAV vectors that can be used to meet specific needs. Literature (Shirley *et al.*, 2020) screened rAAV2-retro, a mutant that can be retrogradely transported along axons in neurons, and obtained AAV-DJ, which can evade serum-neutralizing antibodies and has better liver targeting, with the help of directed evolution. Literature (Ronzitti *et al.*, 2020) discusses that the current directed evolution of AAV has led to a more compact and intelligent construction of mutant libraries by virtue of protein structure analysis and computational prediction and applies the SCHEMA method to the AAV-based Cap gene to optimize the AAV gene iteratively to meet specific needs. SCHEMA approach to DNA reorganization-based mutant library construction to obtain AAV-SCH9 mutants that can target neural stem cells in the subventricular zone. Researchers in the literature (Nidetz *et al.*, 2020) made high-throughput mutant screening possible with the help of DNA barcoding technology and next-generation sequencing. And by combining the directed evolution approach with DNA barcoding technology, multiple types of AAV functional mutants can be efficiently obtained through only one round of *in vivo* screening.

MATERIALS AND METHODS

Materials and reagents

pUC57 plasmid, pds-AAV-CBEGFP plasmid, and E. coli sure were kept in our laboratory. 293T cells were purchased from Shanghai Cell Bank, Chinese Academy of Sciences, restriction endonucleases Notl, Xbal and S1 nuclease, and T4 ligase were purchased from Fermentas (Kishimoto and Samulski, 2022; El Andari and Grimm, 2021). gold view dye, Ta q enzyme was purchased from Solarbio, KODase was purchased from TOYOBO, agarose powder was purchased from Biowest fetal bovine serum was purchased from Cibico, PEI was purchased from ployscience and the rest of the reagents were domestic analytical purity or above (Schmidt *et al.*, 2023). Nucleic acid molecular quality standard DL5000 Marker was purchased from Takara, plasmid extraction kit and gel recovery kit were purchased from Axygen, and cycle pure kit was purchased from Omega. The AAV-TR Expression cassette was synthesized by Suzhou Jinwei Zhi Biotechnology Co. and the PCR primers were synthesized by Shanghai Sangong Bioengineering Technology Service Co (Tran *et al.*, 2020).

Design and synthesis of AAVITR microcarrier sequences

According to the gene structure characterization of AAV, fig. 1 shows the AV-TR single-stranded gene expression vector. The AAVITR sequence is at both ends, and between the left and right ITR sequences are the linear expression cassettes of the exogenous genes, which are CMV enhancer, Chicken Bactin promoter, Multiple cloning site, and SV40-Ploy (A) in order. The AAVITR Expression cassette sequence was placed in the Multiple cloning site of the pUC57 plasmid, enzymatic sites at both ends, to facilitate amplification and preparation of the microvector and the recombinant plasmid was named pUC57-inivector.

Construction of AAVITR gene expression microvector amplification plasmid

The plasmid pds-AV-CBEGFP was used as a template, and the ECFP sequence was amplified by PCR at about 720 bp, and Clal digestion sites were added at both ends of the PCR primers to facilitate ligation with the vector pUC57-minivector. The vector plasmid pUC57-inivetor was digested with Clal, dephosphorylated at 37°C for 30 min, and the vector DNA fragment was recovered by

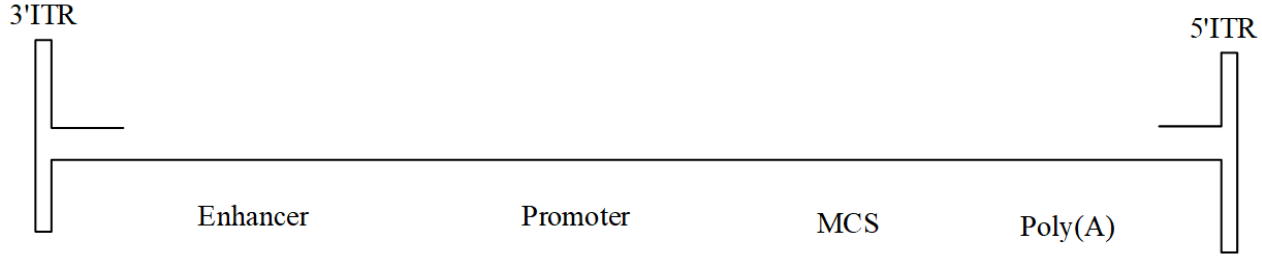

Fig. 1: AAV-TR single-stranded gene expression vector

passing through the column. The PCR product, EGFP sequence, was also digested with ClaI, and the digested product was recovered by passing through the column (Sidonio *et al.*, 2021; Issa *et al.*, 2023). The vector enzyme fragment and the target gene enzyme fragment were ligated under the action of T4 ligase at 22°C for 30 min. The ligated products were transformed into Sure sensory bacteria, and plasmid control and blank control groups were set up, coated with ampicillin-containing antibiotic plates and incubated overnight at 37°C. 16 h later, single colonies appeared on the plates, single colonies on the plates of the experimental group were picked, and the plates were shaken and cultivated in amica-containing LB medium for 16 h at 37°C, 200 r/min, and the plasmid pUC57-inivector EGFP was extracted. The recombinant plasmid was identified by enzymatic digestion and transfection of 293T cells (Buck and Wijnholds, 2020).

Preparation and characterization of AAVITR microvectors pUC57-minivecto

The rEGFP was digested by NotI and the dsminivector-EGFP fragment was recovered by gel. The double-stranded fragment was denatured at 95°C for 5 min and then rapidly cooled on ice for 5 min to obtain the AAVITR microcarrier, and Goldview staining electrophoresis was used to detect the microcarrier fragments obtained by thermal denaturation.S1 nuclease was used to treat the thermally denatured AAVITR microcarrier, and electrophoresis was used to detect whether the microcarrier was degraded or not and the control group was the double-stranded DNA and the plasmid (Pham *et al.*, 2024).

Expression of AAVITR microcarriers in in vitro cells

Human embryonic kidney cell line 293T cells were cultured in DMEM medium containing 10% calf serum, penicillin and streptomycin 100U each in a saturated humidity incubator at 37°C, 5% CO. When the cell growth reached about 80%, the cells were washed twice with PBS solution, 0.25% trypsin was used for digestion at 37°C for 2min and the cells were collected by centrifugation at 800 r/min for 5min and then resuspended with an appropriate amount of medium and then 1/4-1/3 of the cell fluid was taken to continue the culture and the fluid was changed every 1-2 d. The cells were then incubated in the DMEM medium containing 10% calf serum, penicillin, streptomycin, and 100 U each.

Take logarithmic growth phase 293T cells inoculated in 24-well plates, 500 μL per well, density of 2x10'/m, wait for the cell adherence to the wall to grow to a better state, usually 18~24 h, microcarrier DNA transfected cells with PEI, the N/P ratio was 15. PEI-DNA mixture was added to the surface of the 293T cells which had been cleaned with PBS solution, and then an appropriate amount of medium was added, and placed incubated in a saturated humidity incubator at 37°C, 5% CO The expression of CFP was observed by fluorescence microscopy at 24, 48 and 72h after transfection, respectively. After the cells were transfected for 72h, they were digested with 0.25% trypsin, and the cells were collected by centrifugation at 800 r/min for 5 min, and then resuspended with 500 wLPBS solution, and the expression efficiency of GFP was detected by flow cytometry.

Security assessment methods

Cytotoxicity assessment

Cytotoxicity can be assessed in terms of cell viability, apoptosis and cell morphology. Prepare the newly established AAV vector pUC57-inivector-EGFP and the conventional AAV vector, as well as the cell lines to be tested in a good growth state. Cells were inoculated in culture plates at the same density and treated with both vectors at different infection multiplicity MOIs of 10, 50, and 100. For cell viability assessment, the MMY assay was used at three time points, 24, 48 and 72 hours after treatment (Mendell *et al.*, 2021). Specific MMY reagents were added to the cells to fully react with the cells, and the number of live cells was calculated according to the standard curve by detecting the absorbance value of the reagents at specific wavelengths, which in turn led to the cell survival rate, i.e., the number of live cells in the treated group/the number of live cells in the control group × 100%. The apoptosis rate assessment was performed at the same time point and the cells were collected and detected using flow cytometry (Wang *et al.*, 2021). Cells were stained with apoptosis detection reagents such as Annexin V and PI, and the fluorescence signals of the cells were analyzed by flow cytometry to distinguish between different states of cells, and the apoptosis rate, i.e., the number of apoptotic cells as a proportion of the total number of cells, was calculated. Cell morphology evaluation at different time points after the carrier treatment of the cells, the cells were placed under the microscope to observe the morphological changes, including whether the shape is normal, whether there is deformation and floating cells, etc., and compared with the traditional AAV carrier to evaluate the effect of the carrier on the cell morphology and to determine the cytotoxicity.

Immunogenicity assessment

An enzyme-linked immunosorbent assay, called ELISA, is used to quantify cytokine levels. Specifically, samples after carrier treatment, such as cell culture supernatant or tissue homogenate, are collected and added to an enzyme labeling plate pre-coated with a specific antibody, followed by the sequential addition of detection antibody and color developer and the absorbance value is read by the enzyme labeling instrument, and the concentration of cytokines, such as IFN-γ, TNF-α, IL-6, etc., in the samples is calculated based on the standard curve, so as to assess the degree of the body's immune response.

Table 1: Construction and characterization of pUC57-minivector

Enzymatic digestion experiment	Restriction endonucleases used	Expected product size (bp)	Actual observed band size (bp)
Enzymatic digestion 1	BglII	3951 (complete plasmid, assuming no other cut points)	3951
Enzymatic digestion 2	NotI	1239 (AAVITR Expression cassette)	1239
Total		2712 (remaining plasmid fragments)	2712 (remaining plasmid fragments)

Table 2: AAVITR gene table microvector amplification plasmid pUC57-inivector-EGFP

Experiment Name	Specific operation	Results	Resulting data
PCR amplification and characterization of EGFP sequence	PCR amplification of EGFP sequence, recovery by 1.5% agarose gel electrophoresis, 1% electrophoresis identification of PCR products	Specific bands obtained	744bp
Recombinant plasmid construction and identification	The vector plasmid pUC57-inivector and the target gene EGFP sequence were subjected to Clal digestion, and the vector fragment and the target gene fragment were ligated and transformed into Sure receptor to obtain the recombinant plasmid pUC57-inivector EGFP, which was then subjected to Bgll and Clal digestion, respectively.	Different bands obtained	Bgll digestion yielded 4683 bp bands; Clal digestion yielded 744 bp and 3939 bp bands.
Transfection of cells with recombinant plasmids	The recombinant plasmid was transfected into 293T cells for 24h.	Successful expression of target protein	The amount of target protein expressed was 2.5μg/mL, and the transfection efficiency was 60%.

Table 3: Preparation and characterization of AAVITR gene sheet microvectors

Name of experiment	Specific operation	Experimental results	Result data
AAVITR Microvector Preparation and Detection	Prepare AAVITR microvectors by heat denaturation, electrophoresis and Goldview staining.	The migration speed of single-stranded DNA in electrophoresis is significantly faster than that of double-stranded DNA, which indicates that the molecular structure of single-stranded DNA is stretchy and moves more rapidly under the action of electric field. The double-stranded DNA showed green color under UV light, while the single-stranded DNA showed orange color.	The length of single-stranded DNA was 1977 nt, and the length of double-stranded DNA was 3954 nt.
Transfection of cells with AAVITR microcarriers	Transfect 293T cells with AAVITR microvectors.	Target gene EGFP is normally expressed	The target protein expression was 4.5 μg/mL, and the transfection efficiency was 80%.
S1 nuclease treatment (single-stranded)	Treat single-stranded microcarrier with S1 nuclease and observe after electrophoresis.	All degradation	100% degradation rate
S1 Nuclease treatment (double-stranded)	Double-stranded DNA was treated with S1 nuclease and visualized after electrophoresis.	No degradation	0% degradation
S1 Nuclease treatment (plasmid)	Plasmid was treated with S1 nuclease and observed after electrophoresis	No degradation	0% degradation rate

Table 4: 72-hour fluorescence microscopy first observation of GFP

Transfection material	36h	48h	72h
Plasmids	Strong GFP expression, about 80 cells with clear green fluorescence	Expression is reduced, with about 50 cells fluorescing green	When expression is relatively stable but weaker than the highest expression, about 40 cells fluoresce green
Double-stranded DNA	Some GFP expression, about 30 cells fluoresce green	Maximum GFP expression, approximately 70 cells fluoresce green	Expression is weakened, with about 55 cells fluorescing green
Microcarriers	GFP begins to be expressed, approximately 20 cells fluoresce green	GFP expression continues to increase, with approximately 40 cells fluorescing in green	At highest GFP expression, about 60 cells fluoresce green

Table 5: Cytotoxicity assessment of new AAVITR vectors and conventional AAV vectors

Evaluation Indicators	Specific parameters	Newly established AAV-ITR carrier	Conventional AAV carriers
Cell survival rate	MMY method (MOI10,50,100)	92%,88%,85% (24h,48h,72h)	88%,80%,75% (24h,48h,72h)
Apoptosis	Flow cytometry (MOI10,50,100)	5%,7%,10% (24h,48h,72h)	8%,12%15% (24h,48h,72h)
Cytomorphology	Microscopic observation	Normal morphology, no abnormalities	Slightly deformed, few floating cells

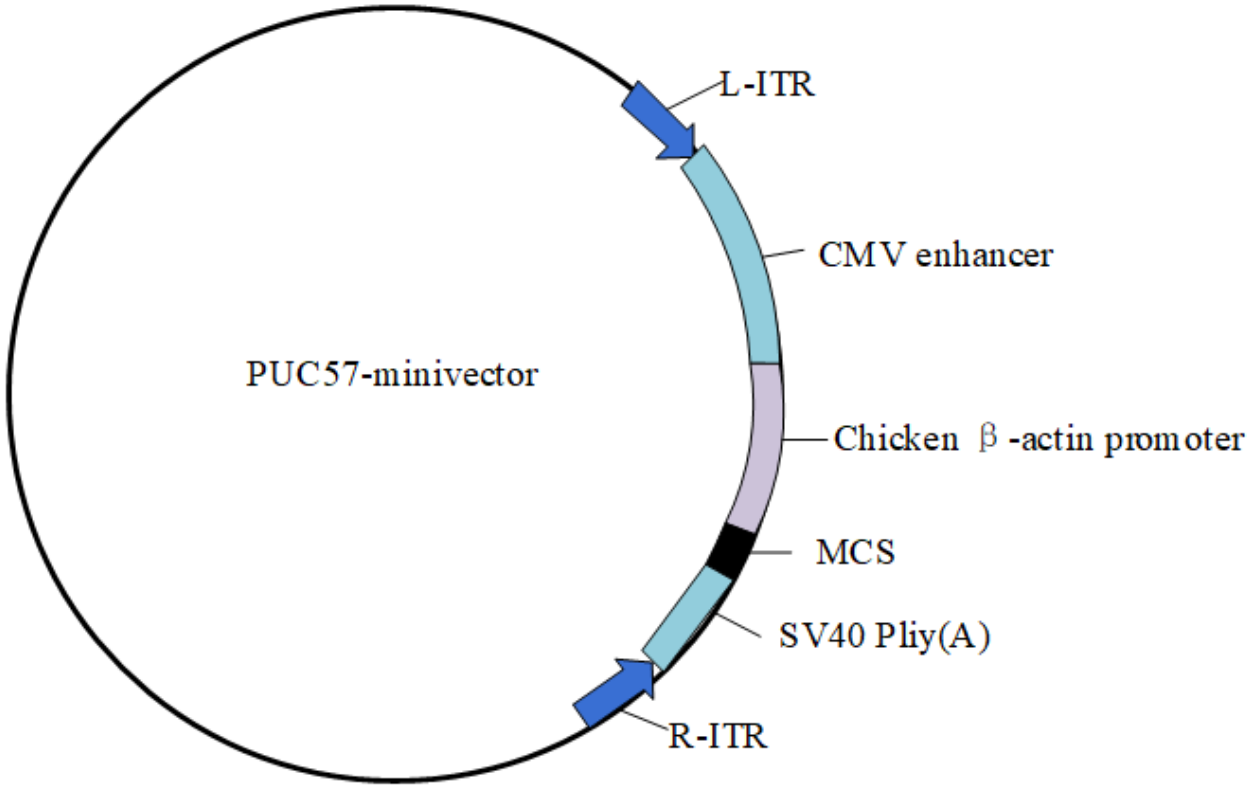

Fig. 2: Construction of pUC57-minivector

Table 6: Comparison of immunogenicity of AAV vector and AAV-ITR microcarrier

Point in time	Indicators	AAV-ITR Micro vector	Traditional AAV carriers	*P*
24 h	Immune cell infiltration	Small number of CD8+ T cells	Almost none	
	Cytokine Levels (pg/mL) - IFN-γ	50 ± 10	20 ± 5	<0.001
	Cytokine Levels (pg/mL) - TNF-α	75 ± 15	35 ± 10	<0.001
	Cytokine Levels (pg/mL) - IL-6	100 ± 20	40 ± 15	<0.001
	Antibody production (ng/mL)-IgG	Not detected (<0.01)	Not detected (<0.01)	
48 h	Immune cell infiltration	Moderate amount of CD8+ T cells	Few CD4+ T cells	
	Cytokine Levels (pg/mL) - IFN-γ	150 ± 30	50 ± 15	<0.001
	Cytokine Levels (pg/mL) - TNF-α	200 ± 40	80 ± 20	<0.001
	Cytokine Levels (pg/mL) - IL-6	250 ± 50	100 ± 30	<0.001
	Antibody production (ng/mL)-IgG	0.1 ± 0.05	Not detected	
72 h	Immune cell infiltration	High-volume CD8+ T cells	Moderate amount of CD4+ T cells	
	Cytokine Levels (pg/mL) - IFN-γ	300 ± 60	100 ± 30	<0.001
	Cytokine Levels (pg/mL) - TNF-α	400 ± 80	150 ± 40	<0.001
	Cytokine Levels (pg/mL) - IL-6	500 ± 100	200 ± 50	<0.001
	Antibody production (ng/mL)-IgG	0.5 ± 0.1	0.05 ± 0.02	0.012
7 days later	Immune cell infiltration	Continuous infiltration	Gradual decrease	
	Cytokine Levels (pg/mL)	Sustained high level	Towards baseline	
	Antibody production (ng/mL)-IgG	1.0 ± 0.2	0.1 ± 0.05	0.025

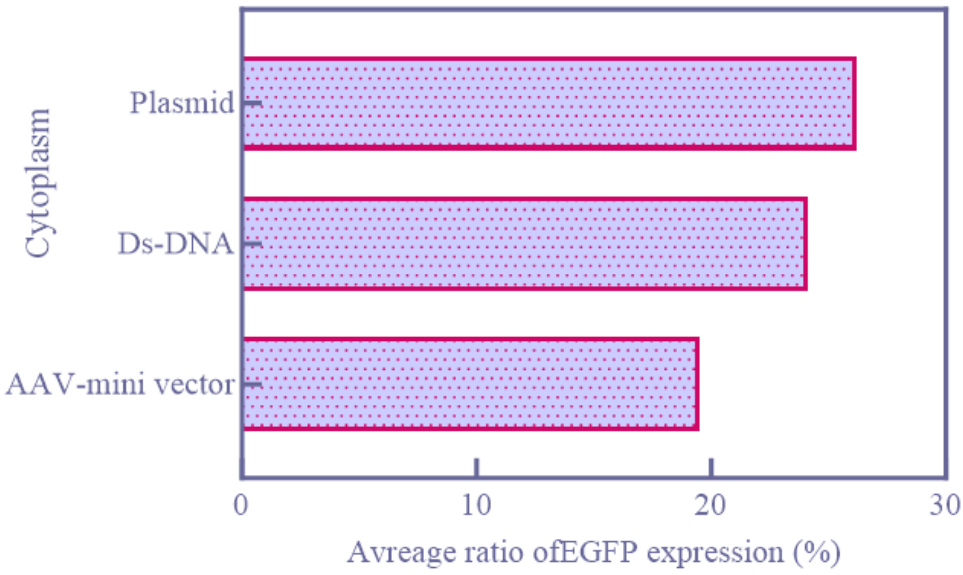

Fig. 3: GFP expression rate determined by flow cytometry

At the same time, the IgG antibody in the sample is detected by using immunoglobulin quantification kits or specific antibody detection techniques and the strength of immunogenicity is further determined by analyzing changes in antibody concentration.

Immune cell infiltration assay

The carrier-treated tissue samples were fixed and sectioned. Then, immunohistochemical staining was applied to bind specific antibodies against immune cell markers such as CD8+ T cells and CD4+ T cells to the corresponding antigens in the tissue sections (Hacker *et al.*, 2020). Then, the stained tissue sections were carefully observed under a microscope, different types of immune cells were counted, and the degree of immune cell infiltration was classified into different grades, such as a small amount, a moderate amount, a large amount, or almost none, according to the number and distribution of

immune cells, to visually assess the state of immune cell infiltration in the tissues (Xu *et al.*, 2021).

STATISTICAL ANALYSIS

Statistical analysis was performed to evaluate the significance of differences between the newly developed AAV-ITR micro vector and conventional AAV vectors. Data were analyzed using GraphPad Prism version 9.0.0 (GraphPad Software, San Diego, CA, USA). Comparisons were made using one-way ANOVA followed by Tukey's multiple comparisons test. P values<0.05 were considered statistically significant.

RESULTS

Construction and characterization of plasmid pUC57-inivector

The AAVITR Expression cassette sequence was cloned on plasmid pUC57 and inserted in the polyclonal site of plasmid pUC57. fig. 2 shows the construction of pUC57-minivector and the recombinant plasmid pUC57-minivector was obtained.

The construction and characterization of pUC57-minivector is shown in table 1 and it can be seen that the expected product size is 3951bp for the complete plasmid when using BglII for the enzyme cut. Assuming that there were no other cutting points, the actual size of the observed band was exactly 3951 bp. This indicates that the BglII digestion reaction was exactly as expected, and the plasmid did not show any other unexpected cuts under the action of this enzyme. In the case of NotI, two products were expected to be produced, namely the 1239bp AAVITR Expression cassette and the 2712bp remaining plasmid fragment. The actual band sizes observed were also 1239bp and 2712bp, as expected. This indicates that the NotI digestion reaction accurately produced the expected two fragments and the reaction proceeded very smoothly.

AAVITR with pUC57-inivector-EGFP

PCR amplified the EGFP sequence, recovered by 1.5% agarose gel electrophoresis and 1% electrophoresis to identify the PCR product, and a 744bp band was obtained. table 2 shows the AAVITR gene episomal micro-vector amplification plasmid pUC57-inivector-EGFP. The vector plasmid pUC57-inivector and the target gene EGFP sequence were ClaI digested and the vector fragment and the target gene fragment were ligated and transformed into Sure sensory state, and the recombinant plasmid pUC57-inivector EGFP was obtained, and the BglII digestion resulted in a band of 4683bp and ClaI digestion resulted in bands of 744bp and 3939bp and the recombinant plasmid was expressed normally after transfection of 293T cells for 24h. The recombinant plasmid was expressed normally after transfection of 293T cells for 24h and the target gene was not expressed. The recombinant plasmid was normally expressed in 293T cells after transfection for 24h.

Preparation and characterization of AAVITR gene sheet micro vectors

The AAVITR micro carriers prepared by thermal denaturation method showed unique properties in several aspects, and the preparation and characterization of AAVITR gene sheet micro carriers are shown in table 3. In the preparation process, the method has the advantages of relatively easy operation and high reproducibility. In terms of physical properties, the length of single-stranded DNA is 1977 nt, while double-stranded DNA is usually twice as long as it, i.e., 3954 nt. Single-stranded DNA migrates significantly faster than double-stranded DNA in electrophoresis because of its more extended molecular structure, which has less resistance under the action of the electric field and moves more rapidly and can be used for rapid isolation and detection in specific experiments. In terms of stability, single-stranded micro carriers are extremely sensitive to S1 nuclease and all of them are degraded after treatment, with a degradation rate of 100%. On the other hand, double-stranded DNA and plasmid DNA showed high stability as no degradation occurred under the same treatment, with a degradation rate of 0%. In terms of transfection performance, after transfecting 293T cells with the micro carrier, the target gene EGFP was able to be expressed normally and the target protein expression was 4.5μg/mL, with a transfection efficiency of 80%, which indicated that the AAVITR micro carrier had some potential for cell transfection, but the transfection effect was affected by a variety of factors.

Expression of AAV-ITR gene episomal micro vectors in 293T cells

Equimolar amounts of plasmid, double-stranded DNA and micro-vector were transfected with PEI in 293T cells, and table 4 shows the observation of GFP by fluorescence microscope first at 72h. The fluorescence microscope first observed the expression of GFP, the plasmid had the highest expression after 36h, the double-stranded DNA had the highest expression after 48h, while the micro vector had the highest expression after 72h.

Fig. 3 shows the GFP expression rate determined by flow cytometry. 72h after transfection of 293T somatic cells with plasmid, double-stranded DNA and micro carrier, trypsin gurgling was collected, and the GFP expression efficiency was detected by flow cytometry, and the micro carrier's expression efficiency of 19.5% was lower than that of the plasmid 26.2% and double-stranded DNA 24.1%.

Safety assessment tests

Cytotoxicity assessment

The cytotoxicity assessment of the new AAVITR vector and the traditional AAV vector is shown in table 5. In

terms of cell survival, the newly established vector showed cell survival rates of 92%, 88% and 85% at different infection multiplicity MOIs of 10, 50 and 100 as well as the time points of 24 hours, 48 hours and 72 hours, respectively, which were higher than those of the traditional vector corresponding to 88%, 80%, and 75%. This indicates that the new vector has a stronger ability to support the survival of cells and can better maintain the normal metabolism and function of cells. As for the apoptosis rate, the new vector was 5%, 7% and 10% at each MOI and time point, which was significantly lower than the 8%, 12% and 15% of the conventional vector. It indicates that the new vector triggers apoptosis to a lesser extent, causing less damage to the cells and helping to maintain the stability of the cell population. In terms of cell morphology, the cells transfected with the newly established vector showed normal morphology and no abnormal performance. In contrast, the cells transfected with the traditional vector showed slight deformation and a small number of floating cells. This further confirmed that the new vector has better biocompatibility and less influence on the structure and function of cells. The newly established AAV vector was superior to the traditional AAV vector in terms of cell survival, apoptosis and cell morphology.

Immunogenicity assessment and detection of immune cell infiltration

At different time points, the new AAV-ITR micro carrier showed significant differences in immune responses with the conventional AAV carrier and a comparison of the immunogenicity of the AAV carrier and the AAV-ITR micro carrier is shown in table 6. At 24 hr, in terms of immune cell infiltration, there was a small amount of CD8+ T-cells infiltrated by the AAV-ITR micro carrier, whereas there was almost no immune cell infiltration by the conventional AAV carrier. In terms of cytokine levels, IFN-γ was 50±10 pg/mL, TNF-α was 75±15pg/mL and IL-6 was 100±20 pg/mL in the AAV-ITR micro carrier, which were significantly higher than those in the conventional AAV carrier, which were 20±5pg/mL, 35±10 pg/mL, and 40±15pg/mL. In terms of antibody production at this stage, neither of them IgG was detected. At 48 hours, there was a moderate amount of CD8+ T cell infiltration with the AAV-ITR micro carrier and a small amount of CD4+ T cell infiltration with the conventional AAV carrier. For cytokines, IFN-γ increased to 150±30 pg/mL, TNF-α to 200±40pg/mL and IL-6 to 250±50 pg/mL in AAV-ITR micro carriers, which were still higher than those of conventional AAV carriers at 50±15pg/mL, 80±20 pg/mL, and 100±30 pg/mL. At this time, AAV-ITR micro carriers produced 0.1±0.05ng/mL of IgG, which remained undetectable in conventional AAV carriers. At 72 hours, there was a large amount of CD8+ T-cell infiltration in AAV-ITR micro carriers, and a moderate amount of CD4+ T-cell infiltration in conventional AAV carriers. Cytokine levels further increased, with IFN-γ reaching 300±60 pg/mL, TNF-α reaching 400±80pg/mL, and IL-6 reaching 500±100pg/mL in the AAV-ITR micro carrier, which were much higher than those in the conventional AAV carrier of 100±30 pg/mL, 150±40 pg/mL, and 200±50 pg/mL. For antibody production, IgG increased to 0.5±0.1ng/mL for the AAV-ITR micro carrier and 0.05±0.02 ng/mL for the conventional AAV carrier. After 7 days, immune cell infiltration was sustained with the AAV-ITR micro carrier and gradually decreased with the conventional AAV carrier. In terms of cytokines, AAV-ITR micro carriers continued to maintain high levels and conventional AAV carriers trended to baseline. For antibody production, IgG reached 1.0±0.2ng/mL for the AAV-ITR micro carrier and 0.1±0.05ng/mL for the conventional AAV carrier. AAV-ITR micro carriers outperformed conventional AAV carriers in terms of immune cell infiltration, cytokine levels and antibody production.

DISCUSSION

This study centered on the design and safety assessment of AAV vectors in gene therapy. In terms of vector design, AAVITR micro vectors and their amplification plasmids were successfully constructed, and the micro vectors were prepared by heat denaturation method. The length of single-stranded DNA was identified as 1977nt and the length of double-stranded DNA was 3954nt and the single-stranded DNA migrated faster than the double-stranded DNA in electrophoresis. The single-stranded micro carrier was sensitive to S1 nuclease, and the degradation rate was up to 100%, whereas the double-stranded DNA and the plasmid DNA had no degradation occurred under the same treatment. After transfecting the micro carriers into 293T cells, the target gene EGFP could be expressed normally, and the expression amount of target protein was 4.5μg/mL and the transfection efficiency was 80%. The safety evaluation test data showed that the newly established AAV-ITR vector performed better in terms of cytotoxicity, with higher cell survival than the traditional vector, lower apoptosis rate, and normal cell morphology at different infection multiplicity and time points. In terms of immunogenicity and immune cell infiltration, the AAV-ITR micro carrier was superior to the conventional AAV vector at different time points. At 72 hours, AAV-ITR micro carriers had a large number of CD8+ T cells infiltrated and cytokine levels further increased, with an IgG content of 0.5±0.1 ng/mL, which was higher than that of the conventional vector of 0.05±0.02ng/mL. 7 days later, AAV-ITR micro carriers showed a sustained infiltration of immune cells and continued high levels of cytokines, in contrast to the conventional vectors. In summary, the AAVITR micro vectors constructed in this study are advantageous in terms of safety and provide a more promising vector option for gene therapy.

The findings of this study have significant implications for the field of gene therapy. The AAV-ITR microvector's reduced immunogenicity and improved safety profile make it a more attractive option for clinical applications, particularly in settings where repeated administration of the vector may be required. The ability to minimize immune responses is critical for the long-term success of gene therapy, as immune reactions can lead to the clearance of therapeutic vectors and reduced efficacy. Moreover, the AAV-ITR microvector's improved transfection efficiency, as demonstrated by the successful expression of the target gene EGFP in 293T cells, suggests that it can effectively deliver therapeutic genes to target cells. This is a crucial aspect of gene therapy, as efficient gene delivery is necessary to achieve therapeutic outcomes. The AAV-ITR microvector's ability to support high levels of gene expression, even at later time points (72 hours post-transfection), indicates its potential for sustained therapeutic effects.

While the results of this study are promising, several areas warrant further investigation. Future research should focus on exploring the detailed mechanisms by which the AAV-ITR microvector achieves its reduced immunogenicity and improved safety profile. This could involve studying the interactions between the microvector and cellular immune receptors, as well as investigating the molecular pathways involved in the cellular response to the vector. Additionally, the AAV-ITR microvector's performance should be evaluated in a broader range of cell types and in vivo models to assess its generalizability and therapeutic potential. Studies should also investigate the long-term stability and functionality of the AAV-ITR microvector in preclinical models to ensure its safety and efficacy over extended periods. Furthermore, the potential for optimizing the AAV-ITR microvector's design to further enhance its performance should be explored. This could involve modifying the vector's sequence or structure to improve its transfection efficiency, reduce immunogenicity, or target specific cell types more effectively.

CONCLUSION

The present study successfully developed a novel AAV vector with enhanced biosafety and efficacy in gene therapy. Our results demonstrate its superiority over conventional vectors in terms of reduced immunogenicity, improved transfection efficiency and favorable safety profiles. This work paves the way for future clinical applications of AAV vectors in gene therapy.

ACKNOWLEDGMENTS

We would like to express our gratitude to all individuals who contributed to the success of this research.

Conflict of interest

The authors have no conflict of interest.

REFERENCES

Au HKE, Isalan M and Mielcarek M (2022). Gene therapy advances: A meta-analysis of AAV usage in clinical settings. *Front. Med. (Lausanne)*, **8**: 809118.

Buck TM and Wijnholds J (2020). Recombinant adeno-associated viral vectors (rAAV)-vector elements in ocular gene therapy clinical trials and transgene expression and bioactivity assays. *Int. J. Mol. Sci.*, **21**(12): 4197.

Bulcha JT, Wang Y, Ma H, Tai PWL and Gao G (2021). Viral vector platforms within the gene therapy landscape. *Signal Transduct. Target. Ther.*, **6**(1): 53.

El Andari J and Grimm D (2021). Production, processing, and characterization of synthetic AAV gene therapy vectors. *Biotechnol. J.*, **16**(1): 2000025.

Ghosh S, Brown AM, Jenkins C and Campbell K (2020). Viral vector systems for gene therapy: A comprehensive literature review of progress and biosafety challenges. *Appl. Biosaf.*, **25**(1): 7-18.

Hacker UT, Bentler M, Kaniowska D, Morgan M and Büning H (2020). Towards clinical implementation of adeno-associated virus (AAV) vectors for cancer gene therapy: Current status and future perspectives. *Cancers*, **12**(7): 1889.

Issa SS, Shaimardanova AA, Solovyeva VV and Rizvanov AA (2023). Various AAV serotypes and their applications in gene therapy: An overview. *Cells*, **12**(5): 785.

Kishimoto TK and Samulski RJ (2022). Addressing high dose AAV toxicity 'one and done'or 'slower and lower' ? *Expert Opin. Biol. Ther.*, **22**(9): 1067-1071.

Li C and Samulski RJ (2020). Engineering adeno-associated virus vectors for gene therapy. *Nat. Rev. Genet.*, **21**(4): 255-272.

Mendell JR, Al-Zaidy SA, Rodino-Klapac LR, Goodspeed K, Gray SJ, Kay CN, Boye SL, Boye SE, George LA, Salabarria S, Corti M, Byrne BJ and Tremblay JP (2021). Current clinical applications of in vivo gene therapy with AAVs. *Mol. Ther.*, **29**(2): 464-488.

Nidetz NF, McGee MC, Tse LV, Li C, Cong L, Li Y and Huang W (2020). Adeno-associated viral vector-mediated immune responses: Understanding barriers to gene delivery. *Pharmacol. Ther.*, **207**: 107453.

Pham Q, Glicksman J and Chatterjee A (2024). Chemical approaches to probe and engineer AAV vectors. *Nanoscale*, **16**(29): 13820-13833.

Pupo A, Fernández A, Low SH, François A, Suárez-Amarán L and Samulski RJ (2022). AAV vectors: The Rubik's cube of human gene therapy. *Mol. Ther.*, **30**(12): 3515-3541.

Ronzitti G, Gross DA and Mingozzi F (2020). Human immune responses to adeno-associated virus (AAV)

vectors. *Front. Immunol.*, **11**: 670.

Schmidt M, Foster GR, Coppens M, Thomsen H, Dolmetsch R, Heijink L, Monahan PE and Pipe SW (2023). Molecular evaluation and vector integration analysis of HCC complicating AAV gene therapy for hemophilia B. *Blood Adv.*, **7**(17): 4966-4969.

Shirley JL, de Jong YP, Terhorst C and Herzog RW (2020). Immune responses to viral gene therapy vectors. *Mol. Ther.*, **28**(3): 709-722.

Sidonio RF Jr, Pipe SW, Callaghan MU, Valentino LA, Monahan PE and Croteau SE (2021). Discussing investigational AAV gene therapy with hemophilia patients: a guide. *Blood Rev.*, **47**: 100759.

Tran NT, Heiner C, Weber K, Weiand M, Wilmot D, Xie J, Wang D, Brown A, Manokaran S, Su Q, Zapp ML, Gao G and Tai PWL (2020). AAV-genome population sequencing of vectors packaging CRISPR components reveals design-influenced heterogeneity. *Mol. Ther. Methods Clin. Dev.*, **18**: 639-651.

Wang Y, Bruggeman KF, Franks S, Gautam V, Hodgetts SI, Harvey AR, Williams RJ and Nisbet DR (2021). Is viral vector gene delivery more effective using biomaterials? *Adv. Healthc. Mater.*, **10**(1): 2001238.

Xu Q, Chen S, Hu Y and Huang W (2021). Landscape of immune microenvironment under immune cell infiltration pattern in breast cancer. *Front. Immunol.*, **12**: 711433.

Zhao H, Lee KJ, Daris M, Lin Y, Wolfe T, Sheng J, Plewa C, Wang S and Meisen WH (2020). Creation of a high-yield AAV vector production platform in suspension cells using a design-of-experiment approach. *Mol. Ther. Methods Clin. Dev.*, **18**: 312-320.

Zhao Z, Anselmo AC and Mitragotri S (2022). Viral vector-based gene therapies in the clinic. *Bioeng. Transl. Med.*, **7**(1): e10258.

Zu H and Gao D (2021). Non-viral vectors in gene therapy: Recent development, challenges and prospects. *AAPS J.*, **23**(4): 78.